

# Quasi-periodic oscillations of Scorpius X-1

Jacob Biemond\*

*Vrije Universiteit, Amsterdam, Section: Nuclear magnetic resonance, 1971-1975*

*\*Postal address: Sansovinostraat 28, 5624 JX Eindhoven, The Netherlands*

Website: <http://www.gravito.nl> Email: [j.biemond@gravito.nl](mailto:j.biemond@gravito.nl)

## ABSTRACT

A comprehensive model for the explanation of quasi-periodic oscillations (QPOs), predicting seven QPO frequencies has recently been presented. In this work it is applied to the observed QPOs of Scorpius X-1. The three highest QPO frequencies are assumed to arise from three circular tori: an inner torus with charge  $Q_i$ , a torus with mass  $m_m$  in the middle and an outer torus with charge  $Q_o$ , whereas the star bears a charge  $Q_s$  (three tori model).

As a consequence of a special interpretation of the gravitomagnetic theory, the three tori are subjected to a total number of four precessions. Expressions for the resulting four gravitomagnetic precession frequencies have recently been presented. It is argued that observation of Lense-Thirring precession need not to become manifest in this approach.

For the Kepler-like frequency of the torus with total mass  $m_m$  the additional contribution of the *gravitational* interaction between a mass element  $dm_m$  and the remaining mass in the torus is explicitly calculated for the first time. The contribution appears to be small.

Predictions of the new model are compatible with two sets of seven QPOs, extracted from observations of Sco X-1. The results are compared with corresponding observations and predictions for four other pulsars and two black holes. Estimates for the Lense-Thirring precessions are also compared with observed QPO frequencies.

## 1. INTRODUCTION

Quasi-periodic oscillations (QPOs) from the pulsar in the low-mass X-ray binary system Scorpius X-1, a Z-source, have been reported by several authors [1–5]. Four QPOs were discovered by Van der Klis *et al.* [1]: two high-frequency QPOs at 1100 Hz and 800 Hz and two low-frequency QPOs at 45 Hz and  $\sim 6$  Hz. Later on, three additional QPOs frequencies were found at 90 Hz, 30 Hz and  $\sim 10$  Hz. [2–5]. In some cases five or six QPOs were simultaneously observed (see refs. [2, fig. 2] and [3, fig. 3], respectively). Finally, Titarchuk *et al.* [5, fig. 1] identified seven different QPOs for Sco X-1 from own and other observations.

Many theoretical models have been proposed to explain the origin of the QPO signals. Usually, these models only deal with the twin high-frequency QPOs. Recently, Lin *et al.* [6] discussed about fifteen of such models, but even the origin of these two high-frequency QPOs remains uncertain. Up to now, the low-frequency QPOs have received relatively less attention, but Titarchuk *et al.* [4, 5] have given a more complete interpretation of the seven observed QPOs for Sco X-1.

Starting from a three tori model in combination with a gravitomagnetic precession model, Biemond [7, 8] recently deduced seven exact formulas for seven QPO frequencies. In this model the three highest QPO frequencies arise from three circular tori around the star, whereas four low-frequency QPOs are generated by a gravitomagnetic precession mechanism. The obtained expressions appeared to be compatible with observations of four pulsars: SAX J1808.4–3658, XTE J1807–294, IGR J00291+5934 and SGR 1806–20 and two black holes: XTE J1550–564 and Sgr A\*.

In this work the latter model will be tested for a high- and low-frequency set of seven previously observed QPO frequencies for Sco X-1 extracted from refs. [1–5]. Six

of the used frequencies have simultaneously measured, whereas the seventh one has been extrapolated.

Compared with other models, two new basic assumptions have been introduced in the deduction of our model. Firstly, it is assumed that pulsars and black holes may bear large stable charges. Starting from the Reissner-Nordström space-time, it has been shown that the required amounts of charge may be bound slightly outside the outer horizon of the so-called ergosphere [8, section 8]. Secondly, for the explanation of four low-frequency QPOs another assumption may be essential: *a special interpretation of the gravitomagnetic theory*, which may be deduced from general relativity [7–12]. In this interpretation the gravitomagnetic field  $\mathbf{B}(\text{gm})$  generated by rotating mass and the electromagnetic induction field  $\mathbf{B}(\text{em})$  due to moving charge are supposed to be equivalent. It is generally accepted that introduction of a gravitomagnetic field is consistent with orthodox general relativity, but the proposed equivalence of  $\mathbf{B}(\text{gm})$  and  $\mathbf{B}(\text{em})$  is not. Application of this special interpretation of the gravitomagnetic field, however, results in the deduction of four new *gravitomagnetic* precession frequencies, which have been identified with four observed low-frequency QPOs [7, 8].

It is noticed, that our interpretation of the gravitomagnetic field also leads to a prediction of the strength of the magnetic field of stars and black holes. Moreover, this approach affects our interpretation of the Lense-Thirring precession. We first consider the first consequence. Identification of the “magnetic-type” gravitational field with a magnetic field results into the so-called Wilson-Blackett formula. This relation applies, e.g., to a spherical star consisting of electrically neutral matter

$$\mathbf{M}(\text{gm}) = -\frac{1}{2}\beta c^{-1}G^{\frac{1}{2}}\mathbf{S}. \quad (1.1)$$

Here  $\mathbf{M}(\text{gm})$  is the gravitomagnetic dipole moment of the star with angular momentum  $\mathbf{S}$ , and  $\beta$  is a dimensionless constant of order unity. Relation (1.1) appears to be approximately valid for many, strongly different celestial bodies and some rotating metallic cylinders in the laboratory as well (see for a review [10] and references therein). The magnetic fields of pulsars have separately been discussed [11]. The angular momentum  $\mathbf{S}$  for a spherical star with mass  $m_s$  and radius  $r_s$  can be calculated from the relations

$$\mathbf{S} = I\boldsymbol{\Omega}_s, \quad \text{and} \quad S = I\Omega_s = \frac{2}{5}f_s m_s r_s^2 \Omega_s, \quad (1.2)$$

where  $\boldsymbol{\Omega}_s$  is the angular velocity vector of the star ( $\Omega_s = 2\pi\nu_s$  is its angular velocity and  $\nu_s$  is its spin frequency),  $I$  is the moment of inertia of the star and  $f_s$  is a dimensionless factor depending on the homogeneity of the mass density in the star. For convenience sake, the value  $f_s = 1$  for a homogeneous mass density will be used in this work.

The value of a gravitomagnetic dipole moment  $\mathbf{M}(\text{gm})$  (or an electromagnetic dipole moment  $\mathbf{M}(\text{em})$ ) can be calculated from

$$\mathbf{M} = \frac{1}{2}R^3\mathbf{B}_p, \quad \text{or} \quad M = \frac{1}{2}R^3B_p. \quad (1.3)$$

Here  $\mathbf{B}_p$  is the magnetic induction field at, say, the north pole of the star at distance  $R$  from the centre of the star to the field point where the field  $\mathbf{B}_p$  may be observed ( $R \geq r_s$ ).

For  $R = r_s$  combination of (1.1), (1.2) and (1.3) yields the following polar field  $\mathbf{B}_p(\text{gm})$

$$\mathbf{B}_p(\text{gm}) = -\frac{2}{5}\beta c^{-1}G^{\frac{1}{2}}m_s r_s^{-1}\boldsymbol{\Omega}_s. \quad (1.4)$$

The minus sign reflects that the vectors  $\mathbf{B}_p(\text{gm})$  and  $\boldsymbol{\Omega}_s$  possess opposite directions for  $\beta = +1$ . Neither the sign nor the value of  $\beta$  follows from the gravitomagnetic theory. It is stressed that  $\mathbf{B}_p(\text{gm})$  at distance  $r_s$  has been derived for an ideal gravitomagnetic dipole

located at the centre of the star. For a homogeneous mass distribution in the star, however, the same result for  $\mathbf{B}_p(\text{gm})$  can be deduced [13, 14].

Furthermore, precession phenomena are another consequence of the special interpretation of the gravitomagnetic theory. The latter theory predicts an angular precession velocity  $\mathbf{\Omega}(\text{gm})$  for an angular momentum  $\mathbf{S}$  of a star or a torus. The following relation then applies to  $\mathbf{\Omega}(\text{gm})$

$$\frac{d\mathbf{S}}{dt} = \mathbf{\Omega}(\text{gm}) \times \mathbf{S}. \quad (1.5)$$

The angular precession velocity  $\mathbf{\Omega}(\text{gm})$  of  $\mathbf{S}$  around direction of the field  $\mathbf{B}(\text{gm})$  from gravitomagnetic origin is given by [7, 10, 12]

$$\mathbf{\Omega}(\text{gm}) = -2\beta^{-1}c^{-1}G^{1/2}\mathbf{B}(\text{gm}), \quad (1.6)$$

where the precession frequency  $\nu(\text{gm})$  is given by  $\nu(\text{gm}) = \mathbf{\Omega}(\text{gm})/(2\pi)$ .

As a first example, the precession of the angular momentum  $\mathbf{S}_m$  of a circular torus with total mass  $m_m$  in the gravitomagnetic field of the star with angular momentum  $\mathbf{S}$  will be considered. According to (1.5), an angular precession velocity  $\mathbf{\Omega}(\text{gm})$  of the component  $\mathbf{S}_m \sin \delta_m$  ( $\delta_m$  is the angle between the directions of  $\mathbf{S}$  and  $\mathbf{S}_m$ ) will occur around  $\mathbf{S}$ . An approximately equatorial orbit for the torus will be adopted, so that  $\delta_m$  is small. By substitution of the equatorial value of the dipolar gravitomagnetic field  $\mathbf{B}_{\text{eq}}(\text{gm}) = -R^{-3}\mathbf{M}(\text{gm})$  into (1.6)  $\mathbf{\Omega}(\text{gm})$  can then directly be found

$$\mathbf{\Omega}_{\text{LT}} = -c^{-2}GR^{-3}\mathbf{S}, \quad \text{or} \quad \nu_{\text{LT}} = -2/5c^{-2}Gm_s\nu_s r_s^2 R^{-3}. \quad (1.7)$$

The precession of the torus with mass  $m_m$  is an example of Lense-Thirring precession. Thus, the obtained result for  $\mathbf{\Omega}(\text{gm})$  is denoted by  $\mathbf{\Omega}_{\text{LT}}$  and the corresponding Lense-Thirring frequency by  $\nu_{\text{LT}}$ . Note that  $\mathbf{B}_{\text{eq}}(\text{gm})$  is approximately constant, when  $\delta_m$  is small. Since  $\mathbf{S}_m \sin \delta_m$  reduces to zero for  $\delta_m = 0$ , however, precession only occurs for  $\delta_m > 0$ .

For  $\delta_m = 90^\circ$  the gravitomagnetic field  $\mathbf{B}(\text{gm})$  in (1.6) is no constant and  $\mathbf{B}(\text{gm})$  has to be integrated over the whole orbit. An averaged result for the Lense-Thirring frequency  $\overline{\nu_{\text{LT}}}$  is then obtained for a circular orbit

$$\overline{\mathbf{\Omega}_{\text{LT}}} = +2c^{-2}GR^{-3}\mathbf{S}, \quad \text{or} \quad \overline{\nu_{\text{LT}}} = 4/5c^{-2}Gm_s\nu_s r_s^2 R^{-3}. \quad (1.8)$$

Note that both in the derivation of (1.7) and (1.8) a dipolar gravitomagnetic field  $\mathbf{B}(\text{gm})$  has been substituted into (1.6). Both relations (1.7) and (1.8) may explain the occurrence of low-frequency QPOs. Recently, Altamirano *et al.* [15] discussed relation (1.8) with respect to the pulsar IGR J17480–2446 in Terzan 5, spinning at a relatively low frequency of  $\nu_s = 11$  Hz. In addition, Homan [16] suggested that Lense-Thirring precession may already have been observed as  $\sim 1$  Hz QPOs in several neutron-star X-ray binaries.

Another situation occurs, when an electromagnetic field  $\mathbf{B}(\text{em})$  is present besides  $\mathbf{B}(\text{gm})$ . Adopting that both fields are equivalent, the resulting total magnetic field  $\mathbf{B}(\text{tot}) = \mathbf{B}(\text{gm}) + \mathbf{B}(\text{em})$  has to be substituted into (1.6). In section 4 we will consider examples of the latter alternative. It is noticed that the proposed equivalence of  $\mathbf{B}(\text{gm})$  and  $\mathbf{B}(\text{em})$  is in contradiction with the analysis of data obtained by the Gravity Probe B satellite and with reported results for the Lense-Thirring precession of the orbit of two LAGEOS satellites. These results are criticized, however (see, e.g., in refs. [12, 13]).

The three tori model from [7], resulting in three high-frequency QPOs  $\nu_i$ ,  $\nu_m$  and  $\nu_o$ , is summarized in section 2. In addition, for the Kepler-like frequency  $\nu_m$  the contribution of the gravitational force between an arbitrary mass element  $dm_m$  in the torus and the

remaining mass of the torus with a total mass  $m_m$  is explicitly calculated for the first time. In section 3 a previously introduced factor  $\beta^*$  is considered. This parameter, depending on the spin frequency  $\nu_s$ , determines the total polar magnetic field  $\mathbf{B}_p(\text{tot})$  of the star. In section 4 the four low-frequency QPOs from gravitomagnetic origin [7],  $\nu_{io}$ ,  $\nu_{mo}$ ,  $\nu_{oi}$  and  $\nu_{mi}$ , are shortly discussed. In section 5 observed QPOs of the pulsar in Sco X-1 are compared with the predictions of the seven QPO model. In section 6 the results for Sco X-1 and four other pulsars are summarized and discussed. In addition, conclusions are drawn.

## 2. THREE TORI MODEL PREDICTING THREE HIGH-FREQUENCY QPOs

The recently proposed model predicting seven QPO frequencies [7, 8] consists of two parts: three high-frequency QPOs are attributed to a three tori model, whereas four low-frequency QPOs may be caused by a gravitomagnetic precession mechanism, summarized in section 4. In this section we deal with the three highest QPO frequencies, which are assumed to arise from three circular tori around the central star. The first frequency  $\nu_i$  is attributed to an *inner* torus containing a total electric charge  $Q_i$ . The sign of the charge of  $Q_i$  is assumed to be opposite to the sign of the total charge  $Q_s$  of the *star*. The second frequency  $\nu_o$  is attributed to an *outer* torus with total charge  $Q_o$  ( $Q_o$  and  $Q_s$  have the same sign). Further, a third torus, containing a total electrically neutral mass  $m_m$  (the subscript m stems from *middle*) is assumed to be present between the two other tori. Thus, it is assumed that  $r_i < r_m < r_o$ .

### 2.1 TWO HIGH-FREQUENCY QPOs: $\nu_i$ , DUE TO THE INNER TORUS WITH CHARGE $Q_i$ , AND $\nu_o$ , DUE TO THE OUTER TORUS WITH CHARGE $Q_o$

By application of Coulomb's law, the gravitation law of Newton and the centrifugal force it can be shown [7], that all forces acting between a point mass  $dm_i$  with charge  $dQ_i$  in the inner torus of radius  $r_i$ , with mass  $m_s$  and charge  $Q_s$  of the star and with a total charge  $Q_o$  in the outer torus of radius  $r_o$ , respectively, can be in equilibrium. Equilibrium is only possible, if the angle between the planes of the tori is not too large. The motion of the tori becomes unstable, when the latter condition is not fulfilled. This instability may (partially) explain the observed frequency and the instability of the high-frequency QPOs  $\nu_i$  and  $\nu_o$ . The expression for  $\nu_i$  is given by [7]

$$\nu_i = \frac{1}{2\pi} \left[ \frac{Gm_s}{r_i^3} \left\{ 1 - \frac{m_s}{m_i} Q_i' (Q_s' - x^2 f Q_o') \right\} \right]^{\frac{1}{2}}, \quad (2.1)$$

where  $m_i$  is the total mass in the inner torus,  $x$  is defined by  $x \equiv r_i/r_o$ ,  $Q_i'$  is defined by the dimensionless quantity  $Q_i' \equiv (G^{\frac{1}{2}} m_s)^{-1} Q_i$ ,  $Q_s'$  by  $Q_s' \equiv (G^{\frac{1}{2}} m_s)^{-1} Q_s$  and so on. In the deduction of (2.1), it has been assumed that the mass and charge densities in both tori are homogeneous. The value of the quantity  $f$  depends on the location of  $dQ_i$  in the inner torus with respect to the outer torus with total charge  $Q_o$ , as has been discussed in refs. [7, 8]. When the inner and outer torus are lying in the same plane,  $f$  reduces to  $f(x)$  in the equilibrium state

$$f(x) = \frac{-2}{\pi x} \left\{ K(x) - \frac{E(x)}{1-x^2} \right\}, \quad (2.2)$$

where  $K(x)$  and  $E(x)$  are complete elliptic integrals of the first kind and second kind, respectively. When both tori are in a bound state but their planes do not coincide, the value of  $f$  varies along the orbit of the inner torus. When  $f$  becomes negative, the tori become unstable. At the least stable situation in the orbit  $f$  reduces to  $f_0 = 0$ . In our calculations we

will approximate the average value of  $f$  over the whole orbit by  $f(\bar{x}) = \frac{1}{2} \{f_0 + f(x)\} = \frac{1}{2} \{0 + f(x)\} = \frac{1}{2} f(x)$ . When the angle between the two tori is not too small, the latter approximation may be reasonable, but for coplanar tori  $f(\bar{x}) = f(x)$ .

It is to be expected that the factor  $m_s/m_i$  on the right hand side of (2.1) is very large. It will be assumed that the difference  $(Q_s' - x^2 f Q_o')$  is very small, so that the charge dependent contribution on the right hand side of (2.1) is small. As a result, the orbital frequency  $\nu_i$  may then be somewhat larger or smaller than the corresponding Kepler frequency  $(2\pi)^{-1}(Gm_s/r_i^3)^{1/2}$ . Instead of using (2.1), we usually apply the following approximate relation in our calculations

$$Q_s \approx x^2 f Q_o. \quad (2.3)$$

This relation is important, for it reduces the number of unknowns like  $x$ ,  $Q_s$  and  $Q_o$  by one.

Following the same method, an analogous equilibrium situation can be found for the same forces acting between a point mass  $dm_o$  with charge  $dQ_o$  in the outer torus of radius  $r_o$ , with mass  $m_s$  and charge  $Q_s$  of the star and with a total charge  $Q_i$  in the inner torus of radius  $r_i$ , respectively. The following expression for the corresponding high-frequency  $\nu_o$  is then obtained [7]

$$\nu_o = \frac{1}{2\pi} \left[ \frac{Gm_s}{r_o^3} \left\{ 1 - \frac{m_s}{m_o} Q_o' (Q_s' + g Q_i') \right\} \right]^{1/2}, \quad (2.4)$$

where  $m_o$  is the total mass in the outer torus and  $Q_o'$  is defined by the dimensionless quantity  $Q_o' \equiv (G^{1/2} m_s)^{-1} Q_o$ , and so on. The value of the quantity  $g$  depends on the location of  $dQ_o$  in the outer torus with respect to the inner torus with total charge  $Q_i$ . It has also been discussed in refs. [7, 8]. When the inner and outer torus are lying in the same in the same plane,  $g$  reduces to  $g(x)$  in the equilibrium state

$$g(x) = \frac{2}{\pi} \left\{ \frac{E(x)}{1-x^2} \right\}, \quad (2.5)$$

where  $E(x)$  is a complete elliptic integral of the second kind. When both tori are in a bound state but their planes do not coincide, the value of  $g$  varies along the orbit of the outer torus. At the least stable situation in the orbit  $g$  reduces to  $g_0$ . In our calculations we will approximate the average value of  $g$  over the whole orbit by  $\bar{g}(\bar{x}) = \frac{1}{2} \{g_0 + g(x)\}$ . When the angle between the two tori is not too small, the latter approximation may be reasonable, but for coplanar tori  $\bar{g}(\bar{x}) = g(x)$ .

It is to be expected that the factor  $m_s/m_o$  on the right hand side of (2.4) is large. In this work it will be assumed that the sum  $(Q_s' + g Q_i')$  is small, so that

$$Q_s \approx -g Q_i. \quad (2.6)$$

As a result, the orbital frequency  $\nu_o$  may thus deviate from the corresponding Kepler frequency  $(2\pi)^{-1}(Gm_s/r_o^3)^{1/2}$ . Relation (2.6) is important, for it reduces the number of unknowns like  $g$ ,  $Q_s$  and  $Q_i$  by one.

It is noticed that Coriolis forces (compare with ref. [4]), Lorentz forces and the gravitational attraction between the masses  $m_i$  and  $m_o$  in the tori have been neglected in the deduction of the results (2.1 and (2.4) in this section. Moreover, no general relativistic effects have been taken into account. Starting from a Kerr-Newman space-time, Aliev and Galtsov [17] considered the latter effects for the binary system of a charged star and a charged point mass moving in a circular orbit around that star. For these reasons and more, the results in this section have to be considered as a first order approximation.

## 2.2 THIRD HIGH-FREQUENCY QPO: $\nu_m$ , DUE TO THE MIDDLE TORUS

Furthermore, the orbital frequency  $\nu_m$  for a point mass  $dm_m$  in a circular orbit of radius  $r_m$  around a star with mass  $m_s$  and angular momentum  $S$  can be shown to be (compare with, e.g., Aliev and Galtsov [17])

$$\nu_m = \frac{1}{2\pi} \left( \frac{Gm_s}{r_m^3} \right)^{1/2} \frac{1}{1 + \frac{S}{c^2 m_s} \left( \frac{Gm_s}{r_m^3} \right)^{1/2}} = \frac{1}{2\pi} \left( \frac{Gm_s}{r_m^3} \right)^{1/2} f_s. \quad (2.7)$$

It is noticed that relation (2.7) applies to prograde motion of  $dm_m$  around the star in the equatorial plane. For pulsars the relativistic factor  $f_s$  in (2.7) depending on the angular momentum  $S$  usually approaches unity value, so that  $\nu_m$  becomes equal to the Kepler frequency  $\nu_K$ .

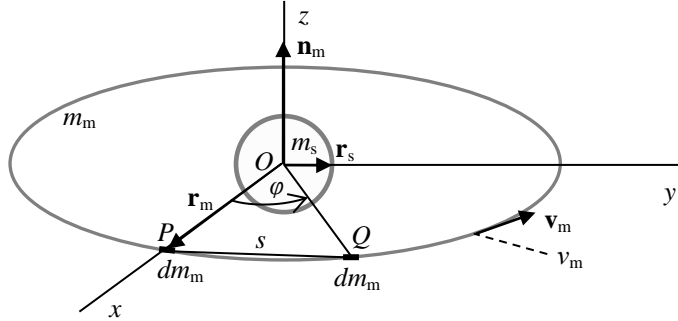


Figure 1. A circular torus of radius  $r_m$  containing a total mass  $m_m$  (grey) is moving around a star of radius  $r_s$  and with a mass  $m_s$  (grey). The unit vector of the normal perpendicular to the plane of the torus is given by  $\mathbf{n}_m$  and coincides with the  $z$ -axis. The velocity of a mass element  $dm_m$  in the torus is given by  $\mathbf{v}_m$  and its frequency by  $\nu_m$ . The mass elements  $dm_m$  at points  $P$  and  $Q$  are separated by a distance  $s$ , whereas  $\varphi$  is the angle between  $OP$  and  $OQ$  ( $O$  is the origin of the  $xyz$ -frame). In this section the net gravitational force lying along the line  $OP$  is calculated.

The result of (2.7) has been deduced for a point mass  $dm_m$  moving in a circular orbit of radius  $r_m$  around a star with mass  $m_s$ . We will now consider the case of a torus of radius  $r_m$  with a total mass  $m_m$  (see figure 1). Especially, we want to calculate the contribution of the gravitational force between a mass element  $dm_m$  located at point  $P$  and the remaining mass in the torus with a total mass  $m_m$ . For symmetry reasons only a net gravitational force acting on  $dm_m$  along the line  $OP$  survives. The calculation is started by considering the following Newtonian forces: the force between the mass element  $dm_m$  located at point  $P$  and the mass  $m_s$  of the star and the force between the mass element  $dm_m$  located at point  $P$  and the mass element  $dm_m$  located at point  $Q$ . When the centrifugal force is also included, the following relation can be obtained in the non-relativistic case

$$\frac{dm_m v_m^2}{r_m} = \frac{dm_m G m_s}{r_m^2} + \frac{dm_m G dm_m}{s^2} \{ \cos(90^\circ - \frac{1}{2}\varphi) \}, \quad (2.8)$$

where  $v_m$  is the velocity of an arbitrary mass element  $dm_m$  moving in the circular orbit of radius  $r_m$ . Since  $\cos(90^\circ - \frac{1}{2}\varphi) = s/(2r_m)$  and  $s = r_m \{ 2(1 - \cos\varphi) \}^{1/2}$ , equation (2.8) can be rewritten as

$$v_m^2 = \frac{Gm_s}{r_m} \left[ 1 + \frac{dm_m}{2\{2(1-\cos\varphi)\}^{1/2}m_s} \right]. \quad (2.9)$$

The following relation applies to a homogeneous mass distribution in the torus with total mass  $m_m$

$$dm_m = \frac{m_m}{2\pi} d\varphi. \quad (2.10)$$

Substitution of (2.10) into (2.9), followed by integration over  $\varphi$  from  $\varphi = \delta\varphi$  to  $\varphi = 2\pi - \delta\varphi$ , leads to the following expression for the high-frequency  $v_m$

$$v_m = \frac{1}{2\pi} \left[ \frac{Gm_s}{r_m^3} \left\{ 1 - \frac{m_m}{2\pi m_s} \ln \left( \operatorname{tg} \frac{\delta\varphi}{4} \right) \right\} \right]^{1/2}. \quad (2.11)$$

Note that for small values of  $\delta\varphi$  the second term on the right hand side of (2.11) is positive. The gravitational attraction between mass element  $dm_m$  at point  $P$  and the remaining mass  $m_m$  in the torus lead to a larger value of the frequency  $v_m$ . The minimum distance  $\delta r = r_m \delta\varphi$  may be put equal to the distance between, e.g., two hydrogen atoms. So,  $\delta r$  is about  $10^{-8}$  cm, whereas  $r_m$  is of the order of the radius of a pulsar, e.g.,  $r_m = 2r_s = 2 \times 10^6$  cm, resulting into a minimum value for  $\operatorname{tg}(\delta\varphi/4)$  of  $1.25 \times 10^{-15}$ . Introduction of this value into the quantity  $m_m/(2\pi m_s) \ln(\operatorname{tg} \delta\varphi/4)$  yields  $-5.5(m_m/m_s)$ . Since the ratio  $(m_m/m_s)$  is usually very small, the contribution  $m_m/(2\pi m_s) \ln(\operatorname{tg} \delta\varphi/4)$  on the r.h.s. of (2.11) will be small compared to unity value and may be neglected.

For the approximated expression (2.11) the high-frequency QPO frequency  $v_m$  for the torus with mass  $m_m$  then coincides with the Kepler frequency  $v_K$ , whereas the radius  $r_m$  can be approximated by the Kepler radius  $r_K$

$$r_m \approx r_K = \left\{ \frac{Gm_s}{(2\pi v_m)^2} \right\}^{1/3}. \quad (2.12)$$

Note that none of the high-frequency QPOs  $v_i$  of (2.1),  $v_m$  of (2.11) or  $v_o$  of (2.4) depends on the spin frequency  $v_s$  of the star. In next section its influence is briefly reviewed (see [7, 8]).

### 3 PARAMETER $\beta^*$

When both a magnetic field  $\mathbf{B}_p(\text{gm})$  from gravitomagnetic origin and a magnetic induction field  $\mathbf{B}_p(\text{em})$  from electromagnetic origin are present at the north pole of the pulsar, the total polar magnetic field  $\mathbf{B}_p(\text{tot})$  is given by

$$\mathbf{B}_p(\text{tot}) = \mathbf{B}_p(\text{gm}) + \mathbf{B}_p(\text{em}). \quad (3.1)$$

According to (1.4), the direction of  $\mathbf{B}_p(\text{gm})$  is antiparallel to  $\boldsymbol{\Omega}_s$  for  $\beta = +1$ . It appears helpful to define the following dimensionless quantity  $\beta^*$  (see ref. [11])

$$\mathbf{B}_p^{\parallel}(\text{tot}) = \beta^* \mathbf{B}_p(\text{gm}). \quad (3.2)$$

When the total field  $\mathbf{B}(\text{tot})$  is from gravitomagnetic origin only,  $\mathbf{B}_p(\text{em}) = 0$ , and  $\beta^*$  reduces to  $\beta^* = 1$ . As a rule, measurements yield  $B(\text{tot})$ , so that only an estimate for  $\beta^*$  can be

obtained.

Several contributions to the field  $\mathbf{B}_p^{\parallel}(\text{em})$  at the north pole of a star have been calculated in ref. [7]. First, a contribution  $\mathbf{B}_p^{\parallel}(\text{em}) = \mathbf{B}_p^{\parallel}(Q_s)$  is generated by the charge  $Q_s$  in the star of radius  $r_s$  and spin frequency  $\nu_s$ . A second contribution  $\mathbf{B}_p^{\parallel}(\text{em}) = \mathbf{B}_p^{\parallel}(Q_i)$  is generated by the charge  $Q_i$  moving in the circular torus of radius  $r_i$ . A third contribution  $\mathbf{B}_p^{\parallel}(Q_o)$  arises from charge  $Q_o$  moving in the circular torus of radius  $r_o$ . Choosing a value  $\beta = +1$ , combination of the gravitomagnetic contribution of (1.4) and the three contributions to  $\mathbf{B}_p^{\parallel}(\text{em})$  leads to the following expression for the parameter  $\beta^*$  (see ref. [7])

$$\beta^* = 1 + \beta_{\text{current}}^* - Q_s' - \frac{1}{2} Q_i' \frac{\nu_i}{\nu_s} \frac{r_i^2/r_s^2 \cos \delta_i}{(1+r_i^2/r_s^2)^{3/2}} - \frac{1}{2} Q_o' \frac{\nu_o}{\nu_s} \frac{r_o^2/r_s^2 \cos \delta_o}{(1+r_o^2/r_s^2)^{3/2}}, \quad (3.3)$$

where  $\delta_i$  is the angle between the direction of the rotation axis  $\mathbf{s} = \mathbf{\Omega}_s/\Omega_s$  of the star and the unit vector  $\mathbf{n}_i$  along the direction of the rotation axis of the torus with total charge  $Q_i$  and so on. Quantities like  $Q_s'$  are again defined by  $Q_s' \equiv (G^{1/2} m_s)^{-1} Q_s$  and so on. Note that the terms in  $Q_s'$ ,  $Q_i'$  and  $Q_o'$  are due to the contributions  $\mathbf{B}_p^{\parallel}(Q_s)$ ,  $\mathbf{B}_p^{\parallel}(Q_i)$  and  $\mathbf{B}_p^{\parallel}(Q_o)$ , respectively. The term  $\beta_{\text{current}}^*$  in (3.3) has been added to account for a possible contribution from toroidal currents in the pulsar. For  $\beta_{\text{current}}^* = -1$  toroidal currents completely compensate the magnetic field from gravitomagnetic origin. A striking property of (3.3) is that it provides a relation between the high-frequency QPOs  $\nu_o$  and  $\nu_i$ , and the spin frequency  $\nu_s$ .

#### 4. FOUR LOW-FREQUENCY QPOs FROM GRAVITOMAGNETIC ORIGIN

If the field  $\mathbf{B}(\text{gm})$  in (1.6) may be identified with an electromagnetic field  $\mathbf{B}(\text{em})$ , the following different gravitomagnetic precession frequencies can be distinguished (The adjective “gravitomagnetic” has been retained, since (1.6) describes the interaction between some *angular momentum* and a magnetic field  $\mathbf{B}(\text{em})$ ). Substitution into (1.6) of the field  $\mathbf{B}(\text{em})$  from the outer torus of radius  $r_o$  and total charge  $Q_o$ , acting on the torus total mass  $m_m$ , yields a precession frequency  $\nu_{mo}$ . The following sequence with respect to the subscripts has been used: the first subscript  $m$  in  $\nu_{mo}$  stems from *middle* and the last subscript  $o$  from *outer*. The mass  $m_m$  in the torus of radius  $r_m$  in the *middle* experiences the action from the charge  $Q_o$  in the *outer* torus ( $r_o > r_m$ ). Likewise, substitution into (1.6) of the field  $\mathbf{B}(\text{em})$  from the charge  $Q_i$  in the torus of radius  $r_i$ , acting on mass  $m_m$ , yields a frequency  $\nu_{mi}$ . In addition, substitution of the field  $\mathbf{B}(\text{em})$  from charge  $Q_o$ , acting on the mass  $m_i$  in the torus of radius  $r_i$  and charge  $Q_i$ , yields a frequency  $\nu_{io}$ . Further, substitution of the field  $\mathbf{B}(\text{em})$  from charge  $Q_i$ , acting on the mass  $m_o$  in the torus of radius  $r_o$  and charge  $Q_o$ , yields a frequency  $\nu_{oi}$ . Thus, a total of four precession frequencies are obtained.

The derivation of the four precession frequencies has been given in ref. [7, sections 3 and 4]. Here we only give the results and some additional remarks. As a first example, the precession frequency  $\nu_{mo}$  of the torus with total mass  $m_m$ , due to the total charge  $Q_o$  in the torus of radius  $r_o$ , is given by

$$\nu_{mo} = -Q_o' \frac{2Gm_s}{c^2 r_o} \nu_o g(x_o) \cos \delta_m \cos \delta_o, \quad (4.1)$$

where  $Q_o'$  is again defined by  $Q_o' \equiv (G^{1/2} m_s)^{-1} Q_o$ . The frequency of the charge  $Q_o$  in the torus of radius  $r_o$  is given by  $\nu_o$  (see (2.4)) and  $x_o$  is defined by  $x_o \equiv r_m/r_o$ . In addition,  $\delta_m$  and  $\delta_o$  are the angles between the direction of the rotation axis of the star  $\mathbf{s} = \mathbf{\Omega}_s/\Omega_s$  and the unit vectors  $\mathbf{n}_m$  and  $\mathbf{n}_o$  along the directions of the rotation axes of the tori with total mass  $m_m$  and total charge  $Q_o$ , respectively. The minus sign in (4.1) means that the angular precession velocity  $\mathbf{\Omega}_{mo}$  ( $\Omega_{mo} = 2\pi\nu_{mo}$ ) is counter-clockwise around  $\mathbf{n}_o$  for  $\beta = +1$  and a

positive charge  $Q_o$ . The function  $g(x_o)$  in (4.1) has been analogously defined to  $g(x)$  in (2.5).

Moreover, the charge  $Q_o$  in the outer torus of radius  $r_o$  acts on the mass  $m_i$  in the inner torus of radius  $r_i$  and may generate a precession frequency  $\nu_{io}$

$$\nu_{io} = -Q_o' \frac{2Gm_s}{c^2 r_o} \nu_o g(x) \cos \delta_i \cos \delta_o, \quad (4.2)$$

where  $Q_o'$ ,  $r_o$ ,  $\nu_o$  and  $\delta_o$  are already given in (4.1) and  $x$  is again defined by  $x \equiv r_i/r_o$ . In addition,  $\delta_i$  is the angle between the direction of the rotation axis of the star  $\mathbf{s} = \mathbf{\Omega}_s/\Omega_s$  and the unit vector  $\mathbf{n}_i$  in the direction of the rotation axis of the torus with mass  $m_i$  and charge  $Q_i$ . Note that the quantity  $g(x)$  in (4.2) equals to  $g(x)$  in (2.5).

Furthermore, the precession frequency  $\nu_{mi}$  of the torus with total mass  $m_m$ , due to the total electric charge  $Q_i$  in the torus of radius  $r_i$ , is given by

$$\nu_{mi} = Q_i' \frac{2Gm_s}{c^2 r_m} \nu_i x_i f(x_i) \cos \delta_m \cos \delta_i, \quad (4.3)$$

where  $Q_i'$  is again defined by  $Q_i' \equiv (G^{1/2} m_s)^{-1} Q_i$ . The frequency of the charge  $Q_i$  in the torus of radius  $r_i$  is given by  $\nu_i$  (see (2.1)) and  $x_i$  is defined by  $x_i \equiv r_i/r_m$ . The definitions of the angles  $\delta_m$  and  $\delta_i$  have already been given. The function  $f(x_i)$  in (4.3) has analogously been defined to  $f(x)$  in (2.2).

Finally, the charge  $Q_i$  in the inner torus of radius  $r_i$  acts on the mass  $m_o$  in the outer torus of radius  $r_o$  and may generate a precession frequency  $\nu_{oi}$

$$\nu_{oi} = Q_i' \frac{2Gm_s}{c^2 r_o} \nu_i x f(x) \cos \delta_i \cos \delta_o, \quad (4.4)$$

where all parameters have already been given before. The quantity  $f(x)$  has earlier been defined in (2.2).

Note that the four frequencies  $\nu_{io}$ ,  $\nu_{mo}$ ,  $\nu_{oi}$  and  $\nu_{mi}$  contain the dimensionless quantity  $Gm_s/(c^2 r_o)$  or  $Gm_s/(c^2 r_m)$ . In general, the quantity  $Gm_s/(c^2 r_o)$  is smaller than unity value for pulsars and black holes, so that the frequencies  $\nu_{mo}$  and  $\nu_{io}$  are usually smaller than  $\nu_o$  and may therefore be denoted as low-frequency QPOs. An analogous line of reasoning can be applied to the frequencies  $\nu_{mi}$  and  $\nu_{oi}$  with respect to  $\nu_i$ . Therefore, they can also be characterized as low-frequency QPOs.

In addition, it is noticed that small angles  $\delta_m$ ,  $\delta_o$  and  $\delta_i$  have always been assumed in the derivations of the precession frequencies (4.1), (4.2), (4.3) and (4.4). If all values of  $\delta$  nearly reduce to zero value, prograde motion of  $Q_i$ ,  $m_m$  and  $Q_o$  around  $\mathbf{s} = \mathbf{\Omega}_s/\Omega_s$  takes place. Alternatively, retrograde motion of  $Q_i$ ,  $m_m$  and  $Q_o$  around  $\mathbf{s}$  implies that all values of  $\delta$  are about  $180^\circ$ .

Furthermore, a remark with respect to the relative magnitudes of  $\nu_{mo}$  and  $\nu_{io}$  can be made. Assuming  $r_o > r_m > r_i$ , implies  $x_o > x$ . According to tables 1 in both refs. [7, 8], the quantity  $g(x_o)$  is then larger than  $g(x)$ . When the angles  $\delta_m$  and  $\delta_i$  do not differ too much, it follows from (4.1) and (4.2) that the frequency  $\nu_{mo}$  is larger than  $\nu_{io}$ . Finally, no sign of any of the frequencies  $\nu_i$ ,  $\nu_m$ ,  $\nu_o$ ,  $\nu_{mo}$ ,  $\nu_{io}$ ,  $\nu_{mi}$  and  $\nu_{oi}$  is known, at this moment. For that reason, positive signs for all frequencies will be used in the calculations below.

## 5. COMPARISON QPOs OF SCORPIUS X-1 WITH PROPOSED MODEL

From observations [1–5] of the pulsar in the low mass X-ray binary system Sco X-1 seven QPO frequencies may be extracted. Six centroid frequencies have simultaneously been measured (see [3, fig. 3], whereas the seventh one may be extrapolated from ref. [5].

The seven obtained QPO frequencies have been assigned to the predicted QPO frequencies  $\nu_i$ ,  $\nu_m$ ,  $\nu_o$ ,  $\nu_{mo}$ ,  $\nu_{io}$ ,  $\nu_{mi}$  and  $\nu_{oi}$ , following from our seven QPO model (see sections 2 and 4, and ref. [7]). Keeping in mind the assumption  $r_i < r_m < r_o$  in our model, the three highest frequencies are attributed to  $\nu_i$ ,  $\nu_m$  and  $\nu_o$ , respectively. An estimate of the relative magnitudes of the other four frequencies can often be made, as has been discussed before. Two series of seven QPO frequencies are extracted: a high- and a low-frequency series. The results are summarized in table 1 and 2, respectively.

The seven equations (2.3), (2.6), (2.12), (4.1)–(4.4) contain nine unknowns (i.e., three charges:  $Q_s$ ,  $Q_o$  and  $Q_i$ ; three radii:  $r_o$ ,  $r_m$  and  $r_i$ ; three angles:  $\delta_o$ ,  $\delta_m$  and  $\delta_i$ ). Only the approximate value of  $r_m \approx r_K$  can directly be calculated from (2.12), when the frequency  $\nu_m$  can be assigned and the value of  $m_s$  is known (In the calculations of all pulsars a mass  $m_s = 1.4 m_\odot = 2.7846 \times 10^{33}$  g has been adopted). Therefore, we have arbitrarily chosen one  $\delta$  value,  $\delta_m$ , and have taken  $\delta_i = \delta_o$ . The remaining seven unknown parameters can then be calculated. See for the further procedure ref. [7]. Using the frequencies  $\nu_o$  and  $\nu_i$ , accurate fits could be found between observed and calculated values of  $\nu_{mo}$ ,  $\nu_{io}$ ,  $\nu_{mi}$  and  $\nu_{oi}$  by application of an iteration process. Results have been summarized in table 1 and 2.

Choosing an arbitrary spin frequency like  $\nu_s = 300$  Hz and taking  $\nu_m = 700$  Hz from table 1 for Sco X-1, calculation from (2.7) yields a value  $r_m = 2.131 \times 10^6$  cm ( $f_s = 0.9927$ ) for prograde rotation, instead of  $r_K = 2.126 \times 10^6$  cm from (2.12). It is noticed, that in the calculation of  $r_m$  the expression  $S$  from (1.2) has been used. The calculations in tables 1 and 2, however, are based on radius  $r_K$  from (2.12).

All calculated radii in tables 1 and 2 meet the condition that they are larger than the radius of the relativistic innermost stable circular orbit in the Schwarzschild space-time,  $r_{ISCO} = 6Gm_s/c^2 = 1.24 \times 10^6$  cm.

Table 1. Seven QPO frequencies of the pulsar in Sco X-1 (high-frequency series). Quality factors  $Q$  and integrated fractional r.m.s. amplitudes are added. Relative radii ( $x$ ,  $x_i$  and  $x_o$ ), radii ( $r_i$ ,  $r_K$ , and  $r_o$ ), relative charges  $Q_s'$ ,  $-Q_i'$  and  $Q_o'$  ( $Q'$  is defined by  $Q' \equiv (G^{1/2}m_s)^{-1}Q$ ), factors  $f(\bar{x})$ ,  $f(\bar{x}_i)$ ,  $\bar{g}(\bar{x})$  and  $\bar{g}(\bar{x}_o)$ , and angles  $\delta_i$  and  $\delta_o$  are calculated. For comment see text.

classif. <sup>a</sup>	$\nu^{b,c}$ (Hz)	$Q$	r.m.s. (%)	$x$	$R \times 10^6$ (cm)	$Q'$	$f(\bar{x})^h$	$\bar{g}(\bar{x})^h$	$\delta$ ( $^\circ$ )
$\nu_u/\nu_h$	$\nu_i$ 970	$10^e$ $10^f$	$1.6^e$ $0.8-2.5^e$		$r_i$ 1.67	$-Q_i'$ 0.168			$\delta_i$ 3.9
$\nu_K$	$\nu_m$ 700	$7^f$	$0.9-1.2^g$		$r_K$ 2.13	$Q'$ 0			$\delta_m$ 9
$\nu_s$ ?	$\nu_s$ ?				$r_s$ 1	$Q_s'$ 0.211			
$\nu_{2L}$	$\nu_o$ 94	$2-5^e$	$0.4-1^e$		$r_o$ 2.64	$Q_o'$ 1.87			$\delta_o$ 3.9
$\nu_L$	$\nu_{mo}$ 46	$6^e$ $2-3^g$	$0.4-1^e$ $\sim 1^g$	$x_o$ 0.8050	$r_o$ 2.64	$Q_o'$ 1.87		$\bar{g}(\bar{x}_o)$ 1.69	$\delta_m = 9$ $\delta_o = 3.9$
$\nu_V$	$\nu_{io}$ 34.5			$x$ 0.6335	$r_o$ 2.64	$Q_o'$ 1.87		$\bar{g}(\bar{x})$ 1.26	$\delta_i = \delta_o$ 3.9
$\nu_b$	$\nu_{mi}$ 14			$x_i$ 0.7869	$r_K$ 2.13	$-Q_i'$ 0.168	$f(\bar{x}_i)$ 0.571		$\delta_m = 9$ $\delta_i = 3.9$
$\nu_{SSV}$	$\nu_{oi}$ $4.5^d$	$0.4-2.1^g$	$1-5^g$	$x$ 0.6335	$r_o$ 2.64	$-Q_i'$ 0.168	$f(\bar{x})$ 0.280		$\delta_i = \delta_o$ 3.9
	$\nu_{LT}(m_i)$ 5.3				$R = r_i$ 1.67				
	$\nu_{LT}(m_m)$ 2.6				$R = r_K$ 2.13				

<sup>a</sup> Classification QPO frequencies from ref. [5]. <sup>b</sup> Ibid, from ref. [7]. <sup>c</sup> The centroid frequencies  $\nu$  have been extracted from refs. [1–5]. <sup>d</sup> The value of  $\nu_{oi}$  is an extrapolation from ref. [5]. <sup>e</sup> Ref. [2]. <sup>f</sup> Ref. [18]. <sup>g</sup> Ref. [1]. <sup>h</sup> Definitions and a discussion of these quantities have been given in sections 2, 4 and ref. [7].

Table 2. *Continued.* Seven QPO frequencies of the pulsar in Sco X-1 (low-frequency series).

classif. <sup>a</sup>	$\nu^{b,c}$ (Hz)	$Q$	r.m.s. (%)	$x$	$R \times 10^6$ (cm)	$Q'$	$f(\bar{x})^h$	$\bar{g}(\bar{x})^h$	$\delta$ ( $^\circ$ )
$\nu_u/\nu_h$	$\nu_i$ 880	$7.7^e$ $8^f$	$2.3^e$ $0.8-2.5^e$		$r_i$ 1.81	$-Q'_i$ 0.192			$\delta_i$ 33
$\nu_K$	$\nu_m$ 575	$5^f$	$0.9-1.2^g$		$r_K$ 2.42	$Q'_K$ 0			$\delta_m$ 9
$\nu_s$ ?	$\nu_s$ ?				$r_s$ 1	$Q'_s$ 0.240			
$\nu_{2L}$	$\nu_o$ 83	$2-5^e$	$0.4-1^e$		$r_o$ 2.86	$Q'_o$ 2.18			$\delta_o$ 33
$\nu_L$	$\nu_{mo}$ 42	$6^e$ $2-3^g$	$0.4-1^e$ $\sim 1^g$	$x_o$ 0.8469	$r_o$ 2.86	$Q'_o$ 2.18		$\bar{g}(\bar{x}_o)$ 1.943	$\delta_m = 9$ $\delta_o = 33$
$\nu_V$	$\nu_{io}$ 23			$x$ 0.6309	$r_o$ 2.86	$Q'_o$ 2.18		$\bar{g}(\bar{x})$ 1.254	$\delta_i = \delta_o$ 33
$\nu_b$	$\nu_{mi}$ 8.1			$x_i$ 0.7449	$r_K$ 2.42	$-Q'_i$ 0.192	$f(\bar{x}_i)$ 0.456		$\delta_m = 9$ $\delta_i = 33$
$\nu_{SSV}$	$\nu_{oi}$ $3^d$	$0.4-2.1^g$	$1-5^g$	$x$ 0.6309	$r_o$ 2.86	$-Q'_i$ 0.192	$f(\bar{x})$ 0.277		$\delta_i = \delta_o$ 33
	$\nu_{LT}(m_i)$ 4.2				$R = r_i$ 1.81				
	$\nu_{LT}(m_m)$ 1.7				$R = r_K$ 2.42				

<sup>a-h</sup> See table 1.

As has been discussed in ref. [7], the quality factors  $Q$  (defined by  $Q \equiv \nu/\Delta\nu$ , where  $\Delta\nu$  is the full-width at half maximum) may depend on the space available for the considered torus. For example, for the inner torus with the high frequencies  $\nu_i = 970$  Hz and 880 Hz the distance  $\Delta r_i$  between innermost stable circular orbit in the Schwarzschild space-time  $r_{ISCO}$  and  $r_i$  increases from  $\Delta r_i \equiv r_K - r_{ISCO} = 0.89 \times 10^6$  cm to  $1.18 \times 10^6$  cm, whereas the  $Q$  values for the inner torus with frequency  $\nu_i$  decrease from 10 in table 1 to 7.7-8 in table 2. For the larger interval of the *upper* frequency  $\nu_u$  ( $\nu_i$  in our notation) of 1070 Hz to 850 kHz the  $Q$  values decrease from 20 to 7 (see ref. [2, fig. 3b]). More in general, the same trend has been discussed by Wang, *et al.* [18] for five Z sources (see their figure 2). Moreover, for the *lower* frequency,  $\nu_m$  in our notation, they found a related trend. For the lower frequencies  $\nu_m = 700$  Hz and  $\nu_m = 575$  Hz the difference  $\Delta r_K \equiv r_o - r_i$  increases from  $0.97 \times 10^6$  cm to  $1.05 \times 10^6$  cm, whereas the  $Q$  values of the frequency  $\nu_m$  decrease from 7 in table 1 to 5 in table 2. Since more space may be available for the outer torus, the  $Q$  values of the frequency  $\nu_o$  are somewhat lower in tables 1 and 2 compared with the  $Q$  values of the frequencies  $\nu_i$  and  $\nu_m$ . Comparable conclusions could be drawn for four other pulsars, as has been discussed in ref. [7]. It is stressed that the explanation for the magnitude of the  $Q$  values is only qualitative. Additional factors may be at work.

It has been found by van der Klis *et al.* [2] that the integrated fractional r.m.s. amplitudes (%) for the *upper* frequency  $\nu_u$  ( $\nu_i$  in our notation) of Sco X-1 decrease for increasing values of  $\nu_i$  (see their fig. 3c). This results may reflect more radiation of the particles for the lower frequency  $\nu_i$ , since the inner torus is then broader and has a higher relative charge  $Q'_i$  (compare tables 1 and 2). High r.m.s. amplitudes have also been found for the outer torus with frequency  $\nu_o$  for pulsars like SAX J1808.4-3658, XTE J1807-294 and IGR J00291+5934 and the stellar black hole XTE J1550-564 (see ref. [7]). A broad outer torus and high values for the relative charge  $Q'_o$  may be relevant factors in the explanation of the observed high r.m.s. amplitudes.

It is noticed that the three tori model has also been applied to the Earth [19] in order to calculate Earth's net charge and the charges of the van Allen belts. The inner and outer van Allen belt are separated with a belt with net zero charge, the so-called electron

slot. Radiation properties of these three belts differ. Data given by Vette [20] show, that the equatorial omnidirectional electron fluxes at different electron energies depend on the radial distance from the Earth. Therefore, the values of the radii  $r_i$ ,  $r_m$  and  $r_o$  of the three tori could be estimated from electron energies of 3 MeV [19].

Another striking feature of the observed QPO frequencies of Sco X-1 is the appearance of the QPO signal at about 6 Hz. Table 1 of ref. [1] shows that  $Q$ -values of the concerning QPO frequency ( $\nu_{oi}$  in our notation) increase from 0.4 to 2, going from 5 to 14 Hz. According to our line of reasoning, decreasing values for  $r_i$  and  $r_o$  (see tables 1 and 2) may lead to an increased value of  $Q$  of frequency  $\nu_{oi}$ .

For equatorial orbits around Sco X-1 (i.e.,  $\delta_m \approx 0$ ), substitution of the value of  $m_s = 1.4 m_\odot$ ,  $r_s = 10^6$  cm and  $\nu_s = 300$  Hz (an arbitrarily chosen value) into (1.7) yields the Lense-Thirring frequencies  $\nu_{LT}(m_i)$  and  $\nu_{LT}(m_m)$  for mass  $m_i$  and  $m_m$  in circular orbits of radii  $r_i$  and  $r_m$ , respectively. The results in tables 1 and 2 show that the values of  $\nu_{LT}(m_i)$  and  $\nu_{oi}$  are then of comparable magnitude. For polar orbits around the pulsar (i.e.,  $\delta_m \approx 90^\circ$ ) the averaged Lense-Thirring frequency  $\bar{\nu}_{LT}$  of (1.8) applies, being twice as large as the corresponding Lense-Thirring frequency  $\nu_{LT}$  from (1.7).

When it is assumed, however, that the gravitomagnetic field  $\mathbf{B}(gm)$  and electromagnetic field  $\mathbf{B}(em)$  are equivalent, the total magnetic  $\mathbf{B}(tot) = \mathbf{B}(gm) + \mathbf{B}(em)$  has to be substituted into (1.6). It is found that for short-period binary pulsars  $\mathbf{B}(tot)$  is usually very small compared with  $\mathbf{B}(gm)$  (see, e.g., ref. [11]). In that case  $\mathbf{B}(tot) \approx 0$  and much smaller values for the Lense-Thirring frequencies from (1.7) in tables 1 and 2 will be obtained.

No value for the parameter  $\beta^*$  for the pulsar of Sco X-1 is yet available. Therefore, in order to be able to calculate  $\beta_{current}^*$  from (3.3), an estimate for  $\beta^*$  must be made. Only for the isolated, millisecond pulsar B1821-24 ( $\nu_s = 328$  Hz) a value  $\beta^* = 2 \times 10^{-5}$  has been extracted from *electron* cyclotron resonance spectral features (see ref. [11]). For that reason, we have used the value  $\beta^* \approx 0$  for Sco X-1 and for other millisecond pulsars. According to (3.2), this assumption also implies that the component of magnetic field at the pole  $B_p^{\parallel}(tot)$  is much smaller than the gravitomagnetic field  $B_p(gm)$ . The latter field for Sco X-1 can be calculated from (1.4). Introducing the values  $m_s = 1.4 m_\odot$ ,  $r_s = 10^6$  cm,  $\nu_s = 300$  Hz and  $\beta = +1$  into (1.4), yields an absolute value of  $B_p(gm) = 1.6 \times 10^{16}$  G.

Substitution of  $\beta^* = 0$  and the other necessary data from tables 1 and 2 into equation (3.3) leads to the following values for  $\beta_{current}^*$  for the high- and low-frequency series, respectively

$$\begin{aligned}\beta_{current}^* &= -1 + 0.21(\text{from } Q_s) - 0.51(\text{from } Q_i) + 0.45(\text{from } Q_o) = -0.85, \\ \beta_{current}^* &= -1 + 0.24(\text{from } Q_s) - 0.44(\text{from } Q_i) + 0.37(\text{from } Q_o) = -0.83.\end{aligned}\tag{5.1}$$

In view of the uncertain values of  $\beta^*$  and  $\nu_s$ , the values of  $\beta_{current}^*$  can only be regarded as an estimate (see refs. [7, 8] and a discussion for short period pulsars in ref. [11]).

Many authors have tried to find correlations between the different QPO frequencies for Sco X-1. For example, van der Klis *et al.* [1] found a strong correlation between  $\nu_{oi}$  and  $\nu_i$ , whereas Wijnands and van der Klis [3] discussed the correlation between  $\nu_{mo}$  and  $\nu_{io}$ . Titarchuk *et al.* [5] investigated the dependence of all seven QPO frequencies on  $\nu_m$ . As an example, the correlation between the QPO frequencies  $\nu_{mi}$  and  $\nu_i$  can be considered. For that reason, equation (4.3) will be rewritten as follows

$$\frac{\nu_{mi}}{\nu_i} = Q_i' \frac{2Gm_s}{c^2 r_m} x_i f(x_i) \cos \delta_m \cos \delta_i, \quad x_i \equiv r_i/r_m \approx r_i/r_K.\tag{5.2}$$

This relation shows that the predicted ratio  $\nu_{mi}/\nu_i$  depends on several largely independent parameters: the relative charge  $Q_i'$ , the radii  $r_i$  and  $r_m$  ( $f(x_i)$  is only a function of  $x_i \equiv r_i/r_m$ ) and the angles  $\delta_m$  and  $\delta_i$ . Comparison of table 1 and 2 shows how much these parameters

vary in equation (5.2). Ratios like  $v_{mi}/v_i$  and  $v_{mo}/v_{mi}$  may, however, be fairly constant, when frequencies vary.

## 6. SUMMARY AND CONCLUSIONS

A comprehensive model of seven observed quasi-periodic oscillations (QPOs) for Sco X-1 has first been given by Titarchuk *et al.* [5]. An alternative model predicting seven QPO frequencies has recently been presented [7, 8]. In this model the three highest QPO frequencies are caused by three tori, as has been summarized in section 2. The remaining four low-frequency QPOs may be generated by a gravitomagnetic precession mechanism, reviewed in section 4.

The three circular tori possess the following properties: the inner torus bears a charge  $Q_i$ , the torus in the middle has an electrically neutral mass  $m_m$  and the outer torus bears a charge  $Q_o$ . It has been shown, that the corresponding QPO frequencies  $v_i$ ,  $v_m$  and  $v_o$  of the binary pulsars SAX J1808.4–3658, XTE J1807–294 and IGR J00291+5934, the soft gamma repeater SGR 1806–20, the white dwarf VW Hyi, the stellar black hole XTE J1550–564 and the supermassive black hole of Sgr A\* are compatible with the three highest frequencies, following the sequence  $v_i > v_m > v_o$ . For the pulsar of Sco X-1 results are summarized in tables 1 and 2. The frequencies  $v_i$ ,  $v_m$  and  $v_o$ , and the radii  $r_i$ ,  $r_m$  (or  $r_K$ ) and  $r_o$  for the other stars are presented in refs. [7, 8]. Results of all considered stars are summarized in table 3. For comparison, the three tori model has also been applied to the Earth in order to calculate Earth's net charge and the charges of the van Allen belts [19].

Note that calculated inner radii for Sco X-1  $r_i = 1.67 \times 10^6$  cm and  $r_i = 1.81 \times 10^6$  cm in table 3 do not much differ from the corresponding Kepler radii  $r_i = 1.71 \times 10^6$  cm and  $r_i =$

Table 3. Summary of frequencies  $v_s$ ,  $v_i$ ,  $v_m$  and  $v_o$  and radii  $r_s$ ,  $r_i$  (or  $r_K$ ) and  $r_o$  for a number of strongly different stars.

Star	$v_s$ (Hz)	$v_i$ (Hz)	$v_m$ (Hz)	$v_o$ (Hz)	$r_s \times 10^6$ (cm)	$r_i \times 10^6$ <sup>e</sup> (cm)	$r_K \times 10^6$ <sup>e</sup> (cm)	$r_o \times 10^6$ <sup>e</sup> (cm)
Pulsars <sup>a</sup>								
Sco X-1 (high freq. series)	300?	970	700	94	1	1.67 (1.71)	(2.13)	2.64 (8.11)
Sco X-1 (low freq. series)	300?	880	575	83	1	1.81 (1.83)	(2.42)	2.86 (8.81)
SAX J1808.4–3658	401	682.4	503.3	189	1	2.22 (2.16)	2.64 (2.65)	3.10 (5.09)
XTE J1807–294	191	544.9	358	134	1	2.69 (2.51)	3.32 (3.32)	3.47 (6.40)
IGR J00291+5934	598.88	66.3	5.3	0.71	1	43.8 (10.2)	55.1 (55.1)	59.0 (211)
SGR 1806–20	0.133	1837	625.5	150.3	1	2.15 (1.12)	2.29 (2.29)	2.51 (5.93)
White dwarf VW Hyi <sup>b</sup>	0.016	0.07305	0.04794	0.02612	650	995 (815)	1080 (1080)	1171 (1618)
Black holes								
XTE J1550–564 <sup>c</sup>	?	268	188	62.9		$(r_g)$ 6.05 (5.40)	$(r_g)$ (6.84) (6.84)	$(r_g)$ 8.28 (14.1)
Sgr A* <sup>d</sup>	?	(mHz) 1.29	(mHz) 0.992	(mHz) 0.751		$(r_g)$ 3.88 (3.58)	$(r_g)$ (4.26) (4.26)	$(r_g)$ 4.56 (5.13)

<sup>a</sup> Adopted mass,  $m_s = 1.4 m_\odot$ , <sup>b</sup>  $m_s = 0.86 m_\odot$ , yielding  $r_{ISCO} = 6Gm_s/c^2 = 0.76 \times 10^6$  cm in Schwarzschild space-time. <sup>c</sup>  $m_s = 9.61 m_\odot$ . In Schwarzschild space-time  $r_{ISCO} = 6Gm_s/c^2 = 6r_g$ . <sup>d</sup> Adopted mass,  $m_s = 3.7 \times 10^6 m_\odot$ . See ref. [8] for comment to  $r_{ISCO}$ . <sup>e</sup> The radii  $r_i$  and  $r_o$  within brackets are Kepler radii calculated from the frequencies  $v_i$  and  $v_o$ .

$1.83 \times 10^6$  cm. All these radii, however, meet the condition that they are larger than the radius of the relativistic innermost stable circular orbit in the Schwarzschild space-time,  $r_{\text{ISCO}} = 6Gm_s/c^2 = 1.24 \times 10^6$  cm. The value of  $r_{\text{ISCO}}$  will decrease by the rotation and by the charge of a pulsar (see, e.g., Dadhich and Kale [21]), but we will not quantify these effects.

The situation inside the pulsar also deserves attention. If the limiting case  $dr/dt = 0$  applies to a certain radius  $r$  smaller than  $r_s$ , then charged particles like protons may be at rest at that radius  $r$ . Application of the condition  $dr/dt = 0$  to the Reissner-Nordström space-time, shows that the proposed amounts of charge may be bound at a spherical shell slightly outside the outer horizon of the so-called ergosphere [8, section 8]. The radius of the outer horizon,  $r_{\text{out}}$ , in the Reissner-Nordström space-time is given by

$$r_{\text{out}} = r_g(1 + \delta) = \frac{Gm_s}{c^2} \left\{ 1 + \left( 1 - Q_s'^2 \right)^{1/2} \right\} = 0.2068 \times 10^6 \left\{ 1 + \left( 1 - Q_s'^2 \right)^{1/2} \right\} \text{cm.} \quad (6.1)$$

Pulsars and black holes may thus bear large stable charges. Although the concerning deduction seems straightforward, it has not yet been noticed to my knowledge. As an example, for Sco X-1 the calculated charge  $Q_s' = 0.211$  of table 1 yields  $r_{\text{out}} = 0.409 \times 10^6$  cm. Note that  $r_{\text{ISCO}}$  is larger than  $r_s$ , whereas  $r_{\text{out}}$  is smaller.

In table 4 the assigned low QPO frequencies  $\nu_{\text{mo}}$ ,  $\nu_{\text{io}}$ ,  $\nu_{\text{mi}}$  and  $\nu_{\text{oi}}$  from (4.1)–(4.4) for five pulsars, including Sco X-1, and two black holes have been summarized. It is usually found that  $\nu_{\text{mo}} > \nu_{\text{io}} > \nu_{\text{mi}} > \nu_{\text{oi}}$ . For the pulsars IGR J00291+5934 and SGR 1806–20 the ratio  $\nu_i/\nu_o$  is much larger than unity value, however, and the sequence changes to  $\nu_{\text{mi}} > \nu_{\text{oi}} > \nu_{\text{mo}} > \nu_{\text{io}}$ . In addition, the relative charges  $Q_i'$ ,  $Q_o'$  and  $Q_s'$  ( $Q_i'$  is defined by  $Q_i' \equiv (G^{1/2} m_s)^{-1} Q_i$  and so on) are given in table 4. It is striking that the values of  $Q_i'$ ,  $Q_o'$  and  $Q_s'$  are lying so close together. The parameters  $\beta^*$  and  $\beta_{\text{current}}^*$  have also been added. For the millisecond pulsars it has been assumed that the total polar magnetic field  $\mathbf{B}_p(\text{tot})$  is small compared with  $\mathbf{B}_p(\text{gm})$ , so that  $\beta^* \approx 0$ . The values of  $\beta_{\text{current}}^*$  can be compared with the asymptotic value  $\beta_{\text{current}}^* = -1$ . Up to now, the obtained values for Sco X-1 are lying closest to this limiting value.

The considered stars in tables 3 and 4 widely differ with respect to the values of the observed frequencies and other properties. Therefore, it is striking that all observed QPOs frequencies can be described by the same unifying model.

Table 4. Summary of frequencies  $\nu_{\text{mo}}$ ,  $\nu_{\text{io}}$ ,  $\nu_{\text{mi}}$  and  $\nu_{\text{oi}}$ , relative charges  $Q_s'$ ,  $Q_i'$  and  $Q_o'$  and parameters  $\beta^*$  and  $\beta_{\text{current}}^*$  for Sco X-1 from tables 1 and 2 in this work and for four other pulsars and for two black holes from refs. [7, 8].

Star	$\nu_{\text{mo}}$ (Hz)	$\nu_{\text{io}}$ (Hz)	$\nu_{\text{mi}}$ (Hz)	$\nu_{\text{oi}}$ (Hz)	$Q_i'$	$Q_o'$	$Q_s'$	$\beta^{*d}$	$\beta_{\text{current}}^{*d}$
Pulsars <sup>a</sup>									
Sco X-1 (high freq.)	46	34.5	14	4.5	-0.17	+1.87	+0.21	$\approx 0$	-0.85
Sco X-1 (low freq.)	42	23	8.1	3	-0.19	+2.18	+0.24	$\approx 0$	-0.83
SAX J1808.4–3658	73.6	46.27	15.02	4.97	-0.24	+1.62	+0.33	$\approx 0$	-0.50
XTE J1807–294	38.3	7.65	3.63	1.67	-0.17	+0.82	+0.26	$\approx 0$	-0.74
IGR J00291+5934	0.0223	0.012	0.052	0.0430	-0.30	+1.77	+0.44	$\approx 0$	-0.56
SGR 1806–20	25.7	17.9	92.7	29.0	+0.13	-0.38	-0.26	+125	+1275
Black holes									
XTE J1550–564 <sup>b</sup>	8.75	5.04	4.090	0.73	-0.070	+0.45	+0.10		
Sgr A <sup>*c</sup>	(mHz) 0.531	(mHz) 0.296	(mHz) 0.130	(mHz) 0.0622	-0.16	+0.49	+0.32		

<sup>a</sup> Adopted mass:  $m_s = 1.4 m_{\odot}$ . <sup>b</sup>  $m_s = 9.61 m_{\odot}$ . <sup>c</sup>  $m_s = 3.7 \times 10^6 m_{\odot}$ . <sup>d</sup> See equation (3.3) and section 3.

As an example, the correlation between the QPO frequencies  $\nu_{mi}$  and  $\nu_i$  in our model has been discussed. The predicted ratio  $\nu_{mi}/\nu_i$  depends on many largely independent parameters, but it is difficult to separate off one of them (see section 5). Many of these ratios appear to be fairly constant, however.

The Lense-Thirring precessions of (1.7) for an equatorial orbit and (1.8) for a polar one deserve special attention. For Sco X-1 and SAX J1808.4–3658 the calculated Lense-Thirring frequencies  $\nu_{LT}(m_i)$  and  $\nu_{LT}(m_m)$  for mass  $m_i$  and  $m_m$  in circular orbits of radius  $r_i$  and  $r_m$ , respectively, may be compatible with observed QPO frequencies (see section 5). In that case, however, two other QPO frequencies ( $\nu_{mo}$  and  $\nu_{io}$  in our notation, see table 4) remain unexplained. For the pulsars IGR J00291+5934 and SGR 1806–20 predictions for  $\nu_{LT}(m_i)$  and  $\nu_{LT}(m_m)$  are much lower than observed QPO frequencies (see ref. [7] and references therein), leaving four low-frequency QPOs unexplained.

Recently, the Lense-Thirring interpretation of low-frequency QPOs has again been considered by Altamirano *et al.* [15]. They reported 35-50 Hz QPOs for the pulsar IGR J17480–2446 in Terzan 5 with spin frequency  $\nu_s = 11$  Hz, but concluded that the QPOs in this range cannot be explained by Lense-Thirring precession. They also cast doubt on the Lense-Thirring interpretation for QPOs in the 35-50 Hz range of other Z-sources with higher spin frequencies, e.g.,  $\nu_s = 300$  Hz (compare with [3, table 1]). Note that our prediction for the QPO frequency  $\nu_{mo}$  of (4.1), not depending on spin frequency  $\nu_s$ , also seems more satisfactory than relations  $\nu_{LT}$  of (1.7) or (1.8), both proportional to  $\nu_s$ . Considering several dipping/eclipsing neutron-star X-ray binaries, Homan [16], suggested, however, that Lense-Thirring precession may already have been observed as  $\sim 1$  Hz QPOs.

In conclusion, for the pulsar in Scorpius X-1 seven QPO frequencies may be extracted from observations [1–5]. As can be seen from tables 1 and 2, the observations are compatible with the recently proposed comprehensive QPO model [7, 8], predicting seven QPO frequencies. In tables 3 and 4 results are summarized of four other pulsars and two black holes, also compatible with this new model.

The deduction of the four low-frequency QPOs starts from the assumption that the gravitomagnetic field, generated by rotating mass is equivalent to the magnetic induction field generated by moving charge [7, 8]. As long as other explanations, like the Lense-Thirring interpretation for low-frequency QPOs [16], are not confirmed, the gravitomagnetic precession model may be an alternative. Another indication for the equivalence of both fields is the approximate validity of the so-called Wilson Blackett law [10, 11]. It is noticed, that the description in terms of a gravitomagnetic field is generally accepted within orthodox general relativity, but the proposed equivalence with the electromagnetic field is not. Moreover, the latter assumption is in contradiction with the analysis of the gravitomagnetic precession rates of four gyroscopes by Gravity Probe B and with the analyses of the Lense-Thirring precession of the orbits of two LAGEOS satellites. The validity of these results has been criticized, however (see, e.g., discussion in refs. [12, 13]). In view of the latter uncertainty, the proposed interpretation of the low-frequency QPOs, may be a viable option.

## REFERENCES

- [1] van der Klis, M., Swank, J. H., Zhang, W. Jahoda, K., Morgan, E. H., Lewin, W. H. G., Vaughan, B. and van Paradijs, J. "Discovery of submillisecond quasi-periodic oscillations in the X-ray flux of Scorpius X-1." *Ap. J.* **469**, L1-L4 (1996).
- [2] van der Klis, M., Wijnands, R. A. D., Horne, K. and Chen, W., "Kilohertz quasi-periodic oscillation peak separation is not constant in Scorpius X-1." *Ap. J.* **481**, L97-100 (1997).
- [3] Wijnands, R. and van der Klis, M., "The broadband power spectra of X-ray binaries." *Ap. J.* **514**, 939-944 (1999).
- [4] Titarchuk, L., Osherovich, V. and Kuznetsov, S., "Timing spectroscopy of quasi-periodic oscillations in the low-mass X-ray neutron star binaries." *Ap. J.* **525**, L129-L132 (1999).

- [5] Titarchuk, L. G., Bradshaw, C. F., Geldzahler, B. J. and Fomalont, E. B., "Normal-Branch quasi-periodic oscillations in Scorpius X-1: Viscous oscillations of a spherical shell near the neutron star." *Ap. J.* **555**, L45-L48 (2001).
- [6] Lin, Y-F, Boutelier, M., Barret, D. and Zhang, S-N., "Studying frequency relationships of kilohertz quasi-periodic oscillations for 4U 1636-53 and Sco X-1: observations confront theories." *Ap. J.* **726**, 74 (12 pp) 2011.
- [7] Biemond, J., "Quasi-periodic oscillations, charge and the gravitomagnetic theory." arXiv:0706.0313v2 [physics.gen-ph], 20 Mar 2009.
- [8] Biemond, J., "Quasi-periodic oscillations, mass and jets of black holes: XTE J1550-564 and Sgr A\*." viXra:astrophysics/1001.0021v1, 18 Jan 2010.
- [9] Biemond, J., *Gravi-magnetism*, 1st ed. (1984). Postal address: Sansovinostraat 28, 5624 JX Eindhoven, The Netherlands. E-mail: [gravi@gewis.nl](mailto:gravi@gewis.nl) Website: <http://www.gewis.nl/~pieterb/gravi/>
- [10] Biemond, J., *Gravito-magnetism*, 2nd ed. (1999). See also ref. [9].
- [11] Biemond, J., "The origin of the magnetic field of pulsars and the gravitomagnetic theory." In: *Trends in pulsar research* (Ed. Lowry, J. A.), Nova Science Publishers, New York, Chapter 2 (2007) (updated and revised version of arXiv:astro-ph/0401468v1, 22 Jan 2004).
- [12] Biemond, J., "Which gravitomagnetic precession rate will be measured by Gravity Probe B?" arXiv:physics/0411129v1 [physics.gen-ph], 13 Nov 2004.
- [13] Biemond, J., "The gravitomagnetic field of a sphere, Gravity Probe B and the LAGEOS satellites", arXiv:0802.3346v2 [physics.gen-ph], 14 Jan 2012.
- [14] Biemond, J., "The gravitomagnetic vector potential and the gravitomagnetic field of a rotating sphere." viXra:astrophysics/1205.0064v1, 15 May 2012.
- [15] Altamirano, D., Ingram, A., van der Klis, M., Wijnands R., Linares, M. and Homan, J., "Low-frequency quasi-periodic oscillation from the 11 Hz accreting pulsar in Terzan 5: not frame dragging." *Ap. J.* **759**, L20-L25 (2012).
- [16] Homan, J., "A possible signature of Lense-Thirring precession in dipping and eclipsing neutron-star low-mass X-ray binaries." *Ap. J.* **760**, L30-L33 (2012).
- [17] Aliev, A. N. and Galtsov, D. V., "Radiation from relativistic particles in nongeodesic motion in a strong gravitational field." *Gen. Rel. Grav.* **13**, 899-912 (1981).
- [18] Wang, J., Chang H. K., Zhang, C. M. Wang, D. H., Chen. L. Qu, J. L and Song, L. M., "Morphological analysis on the coherence of kHz QPOs." *Astrophys. Space Sci.* **342**, 357-364 (2012).
- [19] Biemond, J., "Earth's charge and the charges of the Van Allen belts." viXra:geophysics/1008.0071v1, 25 Aug 2010.
- [20] Vette, J. I., "The AE-8 trapped electron model environment." National Space Science Data Center (NSSDC) World Data Center A for Rockets and Satellites (WDC-A-R&S), 91-24, NASA, Goddard Space Flight Center, Greenbelt, Maryland (1991).
- [21] Dadhich N. and Kale, P. P., "Equatorial circular geodesics in the Kerr-Newman geometry." *J. Math. Phys.* **18**, 1727-1728 (1977).